

The Effect of Pre-Electroacupuncture on Nociceptive Discharges of Spinal Wide Dynamic Range Neurons in Rat

Qingquan Yu, Wanying Cao, Xiaoyu Wang, Wei He, Xiaoyue Sun, Lizhen Chen, Yangshuai Su, Zhiyun Zhang, Xianghong Jing

Institute of Acupuncture and Moxibustion, China Academy of Chinese Medical Sciences, Beijing, People's Republic of China

Correspondence: Zhiyun Zhang; Xianghong Jing, Institute of Acupuncture and Moxibustion, China Academy of Chinese Medical Sciences, 16th Nanxiaojie of Dongzhimennei, Beijing, 100700, People's Republic of China, Email zhangzhiyun@yeah.net; jxhtjb@263.net

Purpose: Spinal wide dynamic range (WDR) neurons are well studied in pain models and they play critical roles in regulating nociception. Evidence has started to accumulate that acupuncture produces a good analgesic effect via activating different primary fibers with distinct intensities. The purpose of the present study was to compare the distinct intensities of pre-electroacupuncture (pre-EA) at local muscular receptive fields (RFs), adjacent or contralateral non-RFs regulating the nociceptive discharges of spinal WDR neurons evoked by hypertonic saline (HS).

Materials and Methods: Spinal segments of electrophysiological recording were identified by neural tracers applied at the left gastrocnemius muscle. The thresholds of A β (T $_{A\beta}$), A δ (T $_{A\delta}$) and C (T $_C$) components of WDR neurons were measured to determine the intensity of pre-EA by extracellular recording. The discharges of WDR neurons induced by distinct intensities of pre-EA and 200 μ L HS (6%) injection in left gastrocnemius muscle of rats were observed by extracellular recording.

Results: The spinal segments of WDR neurons were confirmed in lumbar (L)5–6 area according to the projective segments of dorsal root ganglion. T $_{A\beta}$, T $_{A\delta}$ and T $_C$ of WDR neurons was determined to be 0.5, 1, and 2 mA, respectively. The pre-EA with intensities of T $_{A\beta}$ ($P < 0.05$), T $_{A\delta}$ ($P < 0.05$), T $_C$ ($P < 0.05$) or 2T $_C$ ($P < 0.01$) at ipsilateral adjacent non-RFs significantly reduced the discharges of WDR neurons, while at local RFs only pre-EA of T $_{A\delta}$ ($P < 0.05$), T $_C$ ($P < 0.05$) and 2T $_C$ ($P < 0.01$) could inhibit the nociceptive discharges. In addition, intensity of pre-EA at contralateral non-RFs should reach at least T $_C$ to effectively inhibit the firing rates of WDR neurons ($P < 0.01$).

Conclusion: Pre-EA could suppress nociceptive discharges of WDR neurons and the inhibitory effects were dependent on the distinct intensities and locations of stimulation.

Keywords: pre-electroacupuncture, wide dynamic range neurons, muscular receptive fields, intensity, hypertonic saline

Introduction

The spinal dorsal horn (SDH) is the first station that relays somatosensory afferents. Spinal wide dynamic range (WDR) neurons in the deep laminae (IV-VI) play a critical role in nociception. WDR neurons respond to a wide range of stimulation which transmits innocuous and noxious information through A β -, A δ - and C-fibers.¹ Previous studies showed that the WDR neurons exhibited progressive discharges in a graded manner depending on stimulus intensity, which manifested in an increase of discharge frequency and expansion of receptive fields (RFs).^{2–4} Accordingly, the WDR neurons significantly contribute to the encoding of spatial and qualitative aspects of pain and integration of various afferent inputs.^{5,6}

Acupuncture analgesia (AA) is closely dependent on the stimulating intensities and locations of acupoints,^{7–9} where different types of afferent fibers (A β , A δ and C) were activated. Electro-acupuncture (EA) with low intensity at local acupoint could activate non-nociceptive A β -fiber to elicit segmental analgesia, while systemic analgesia produced by heterotopic EA intervention relies on sufficient activation of noxious A δ - and C-fibers.^{10,11} Therefore, distinct intensities

of EA may exert analgesic effect through different mechanisms. Meanwhile, the preventive analgesic effects of pretreatment of EA (pre-EA) have also been reported in numerous clinical trials and experimental studies.^{12,13} However, the activity of WDR neurons during pre-EA with different intensities remain elusive.

As a group of convergent neurons encoding different stimulus, WDR neurons may integrate acupuncture and pain signals in SDH. Indeed, previous studies suggested that the activities of WDR neurons were greatly relevant to AA and EA intervention was able to inhibit nociceptive discharges of WDR neurons in various pain models.^{14,15} A recent study also showed that EA inhibited spontaneous firing of WDR neurons by activating A-fibers in muscular inflammatory pain in rats.¹⁶ Moreover, EA intervention at homotopic or heterotopic acupoints produced ameliorated effects on visceral pain via suppressing nociceptive discharges of WDR neurons in an intensity-dependent manner.^{17–19} These studies indicated that the inhibitory effects of EA intervention on WDR neurons were closely related to the activation of different afferent fibers. However, there is a lack of consensus about WDR neurons integrating the pre-EA intervention and somatic nociception.

The aim of the present study was to explore whether pre-EA regulates the nociceptive activities of WDR neurons according to different intensities and the locations of intervention. We first identified the intensity thresholds of A β ($T_{A\beta}$), A δ ($T_{A\delta}$) and C (T_C)-components of WDR neurons elicited by EA intervention. Then pre-EA with distinct intensities ($T_{A\beta}$, $T_{A\delta}$, T_C or $2T_C$) was administered at local RFs, adjacent or contralateral non-RFs, respectively. Following the pre-EA intervention, nociceptive discharges of WDR neurons evoked by injection of hypertonic saline (HS) were observed. At last, the effects of pre-EA with different intensities and locations on discharges of WDR neurons were estimated.

Materials and Methods

Animals

Male Sprague-Dawley rats (200 \pm 20 g) were provided by the SPF (Beijing) Biotechnology Co., Ltd. [experimental animal license number: SCXK(JING)2019–0010]. All animals were kept at a constant temperature of 24 \pm 2°C with a 12-h light 12-h dark cycle and with free access to food and water. After a week of adjustable feeding, animals were randomly allocated to the normal, control, model and pre-EA group. The experimental procedures were approved by the Ethics Committee of the Institutional Animal Welfare and Use Committee of Acupuncture and Moxibustion Institute of China Academy of Chinese Medical Sciences. All manipulations were performed in accordance with the recommendations of the Guideline on the Humane Care and Use of Laboratory Animals issued by the Ministry of Science and Technology of the People's Republic of China in 2006.

Microinjection of Neural Tracer

Under respiratory anesthesia with 2% isoflurane (0.5 L/min, RWD Life Science, People's Republic of China), 5 μ L 0.1% cholera toxin subunit B conjugates of Alexa Fluor-488 (AF488-CTB, C34775, Thermo, Germany) was slowly injected into the left gastrocnemius muscle of rats at a depth of 3–7 mm, right at the medial muscle belly. To prevent leakage, the microsyringe remained in place for 1 min after injection, and was then removed.²⁰

Perfusion and Tissue Processing

Three days after injection of neural tracer, the rats were deeply anesthetized intraperitoneally with urethane (1.5 mg/kg) and then transcardially perfused with 250 mL of 0.9% NaCl, followed by 250 mL of cold 4% paraformaldehyde (PFA) in 0.1 M phosphate-buffered solution (PB, pH 7.4). The lumbar (L)1–6 and sacral (S)1 of dorsal root ganglia (DRG) were collected and post-fixed in 4% PFA for 2 h and then cryoprotected in 25% sucrose at 4°C for 24 h. Using a cryostat (Thermo, Microm International FSE, Germany), DRGs were sliced transversely into 40 μ m thick sections and mounted on silane-coated glass slides. After being coverslipped with 50% glycerin, all the labeled neurons in sections were observed and recorded with fluorescent microscope equipped with a digital camera (BX53, Olympus, Japan).²¹

Surgical Exposure of Spinal Cord

After rats were deeply anesthetized intraperitoneally with urethane (1.5 mg/kg), laminectomy was performed at the thoracic (T)12 to L2 to expose the lumbar enlargement (L4-6) of the spinal cord. Carefully removed dura mater of lumbosacral segments of spinal and tightly fixed the corresponding vertebrae in a rigid frame with clamps. Exposed area of spinal cord was covered with warm (37°C) artificial cerebrospinal fluid (CZ0516, Leagene, People's Republic of China) during surgery and recording. A feedback-controlled heating blanket (ALC-HTP, Shanghai Alcott Biotech Co., People's Republic of China) was used to monitor and maintain core body temperature at $37.0 \pm 0.5^\circ\text{C}$.²²

Extracellular Recording of the SDH Neurons

Extracellular recording of SDH neurons was performed at L4-6 segments through a 5 M Ω parylene-coated tungsten microelectrode²³ (575,500, A-M Systems, Sequim, WA, United States) or a microelectrode array²⁴ (ASSY, Lotus Biochips, United States) (Figure 1A and B). After surgery, recording electrodes were inserted perpendicularly into the SDH at a depth of approximately 600–1400 μm from the dorsal surface and 0.3 mm lateral to the central vessel by a micromanipulator (DMA-1510, Narishige, Japan). The reference electrode was placed in the nearby muscle. Signals from parylene-coated tungsten microelectrode were amplified by a preamplifier (AM-1800, AM Systems, Sequim, WA, United States) with a bandwidth of 300 Hz–5 kHz and captured online using the CED 1401-plus data acquisition system and analyzed offline by Spike 2 package software (Cambridge Electronic Devices, Cambridge, United Kingdom). Microelectrode array was attached to the headstage using a custom connector and signals were amplified by a preamplifier (LB-0164-1, Blackrock Microsystems, United States) with a bandwidth of 250 Hz–5 kHz and captured and amplified online by a data acquisition system (Cerebus-128, Blackrock Microsystems, United States).

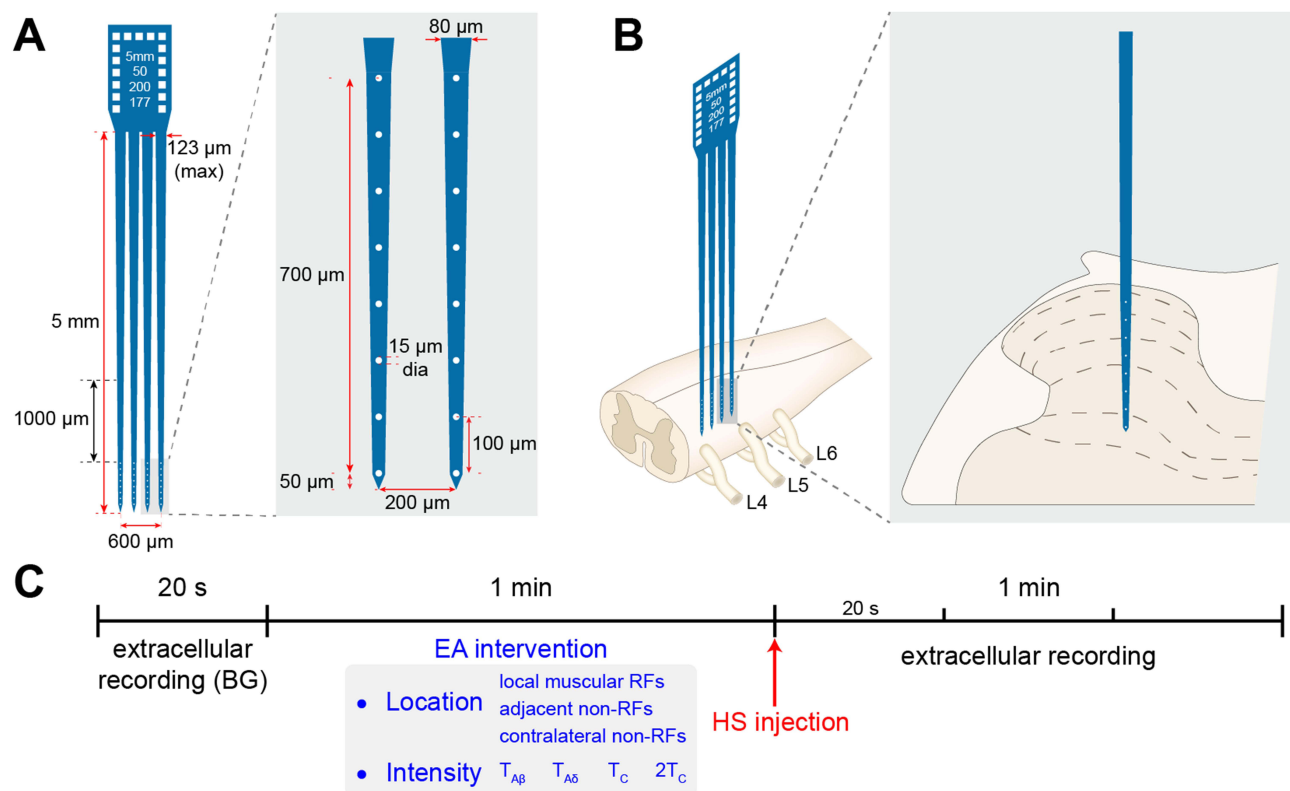


Figure 1 Recording of neurons' activity in the spinal dorsal horn (SDH) by a microelectrode array and experimental procedure.

Notes: (A) Illustration of a microelectrode array with 4 electrodes (750- μm depth, 32 channels). (B) Schematic diagram of recording with microelectrode array and position of microelectrode across Lamina II-VI noted with dotted lines. (C) Experimental timeline. Following 20s recording of background (BG) discharge, distinct intensities ($T_{A\beta}$, $T_{A\delta}$, T_C or $2T_C$) of EA intervention were applied at ipsilateral RFs, adjacent or contralateral non-RFs for 1 min. Immediately after EA intervention, HS was injected at left gastrocnemius muscle (identified as muscular RFs) of rats. Then, the neuronal discharge was recorded for 1 min.

Identification of WDR Neurons and Receptive Fields

WDR neurons were identified by a mechanical press stimulator (ALMEMO2450, Ahlborn, Germany) equipped with a blunt rubber tip 0.5 cm in diameter. The mechanical threshold for escape behavior was measured at gastrocnemius muscle in awakened rats, which was 149.1 ± 13.2 g (3 rats). Therefore, 60 and 200 g were determined as innocuous and noxious stimulation, respectively.²⁵ During extracellular recording, mechanical stimulation was applied at the muscular RFs. Neurons responding to both innocuous and noxious stimulation were identified as WDR neurons. Additionally, to discriminate the responses of WDR neurons between the skin and muscle, local cutaneous afferents were blocked by hypodermic injection of 50 μ L lidocaine hydrochloride (Haerbin sanmashouyaoye Co., People's Republic of China) above the RFs.²⁶ The present study focused on WDR neurons that responded only to pressure of the muscle but not to pinch of the skin.

Identification of Intensity Thresholds Activating A β -, A δ - and C-Components of WDR Neurons

Identification of thresholds was performed at WDR neurons with RFs located at the anterior tibial muscle or the gastrocnemius muscle. Electrical stimulation was delivered through an electrical stimulator (PowerlabFE180, AD Instruments, Australia) at the RFs during extracellular single-unit recording. Intensity of electrical stimulation increased gradually from 0.1 mA (0.5 ms pulse width) until 3 components with corresponding latencies (A β , 0–20 ms, A δ , 20–90 ms, C, 90–300 ms) appeared.²³ Intensity that evoked discharge more than 3 times (6 times in total, 5 s intervals) was identified as threshold of corresponding component (T_{A β} , T_{A δ} or T_C).^{27,28}

EA Intervention

EA intervention was applied at ipsilateral RFs, adjacent or contralateral non-RFs. A pair of stainless steel acupuncture needles (0.18 mm diameter, 13 mm length; Beijing Zhongyan Taihe Medicine Co., People's Republic of China) were inserted into the muscle at a depth of 5 mm. EA intervention was applied with intensity of T_{A β} , T_{A δ} , T_C or 2T_C (0.5 ms pulse width) at a frequency of 2 Hz for 1 min (Figure 1C), which was delivered by an electrical stimulator.

Administration of Saline

6% hypertonic saline (HS) was prepared as noxious stimulus. Immediately after EA intervention was finished, 200 μ L HS was administered through the placement of a 10 cm long PE-10 tube at left gastrocnemius muscle of rats in advance (Figure 1C). Injection was administered at depth of 5–7 mm within 10s. Rats in control group were injected with the same volume of 0.9% NaCl.

Statistical Analysis

All data were expressed as means \pm standard error of the means (SEM). Statistical analysis was performed with SPSS 23 software. The Shapiro–Wilk test was used to evaluate whether these data fit normal distributions. Normally and non-normally distributed data were analyzed via parametric or non-parametric tests, respectively. Differences among multiple groups were analyzed with one-way analysis of variance (ANOVA) test followed by the LSD, SNK, or Dunnett's T3 post hoc test. Differences with $P < 0.05$ were considered significant.

Results

Identification of WDR Neurons with Muscular Receptive Fields

To locate the exact segments of electrophysiological recording, the retrograde neural tracer was injected at left gastrocnemius muscle to identify the relevant sensory innervation. As shown in Figure 2A and B, the sensory neurons labeled by AF488-CTB were distributed from L3 to sacral (S)1 and concentrated at L5-6 DRGs, indicating that the sensory inputs of gastrocnemius muscle mainly projected to L5-6 SDH. Therefore, recording of WDR neurons was performed at L5-6 segments of the SDH. WDR neurons were identified by mechanical stimulation, including innocuous 60 g and noxious 200 g pressure as well as innocuous brushing at left gastrocnemius muscle and anterior tibial muscle.

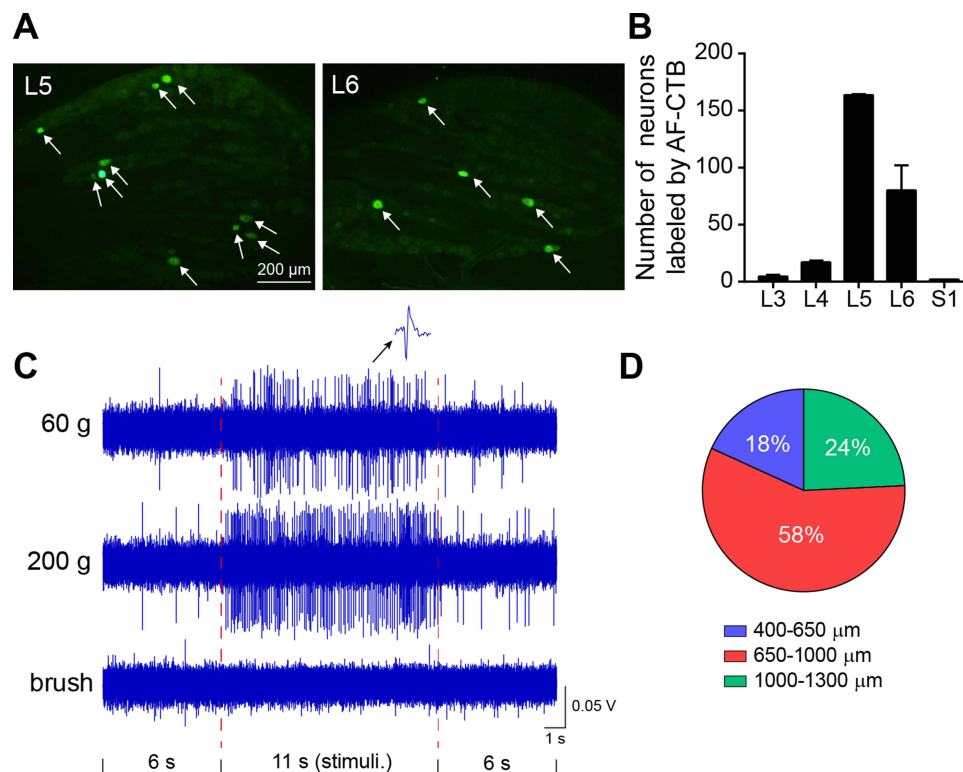


Figure 2 General properties of WDR neurons with receptive fields (RFs) at left gastrocnemius muscle.

Notes: (A) Representative images of retrogradely labeled primary sensory neurons (white arrows) in lumbar (L)4 and L5 dorsal root ganglia (DRG) associated with left gastrocnemius muscle. (B) The number of labeled sensory neurons in L3-6 and sacral (S)1 DRGs (n=3). (C) Representative discharge mode of WDR neurons evoked by 60 and 200 g pressure on muscular RFs and brush on local skin. (D) Percentages of WDR neurons distributed among different depths of SDH (106 neurons from 70 rats). All data were presented as means \pm SEM.

Neurons responded to both innocuous and noxious pressure but not brushing were identified as WDR neurons with muscular RFs (Figure 2C).^{16,25} A total of 106 WDR neurons were recorded from 70 rats. Most WDR neurons were distributed at a depth of 650–1300 μ m below the dorsal surface of the spinal cord, corresponding to laminae IV–VI of the SDH (Figure 2D).

Thresholds of A β -, A δ - and C-Components of WDR Neurons

Typical discharge of WDR neurons to multiple types of primary sensory inputs can be separated into A β -, A δ - and C-components by the corresponding latencies (0–20, 20–90 and 90–300 ms, respectively).²³ To determine the activation thresholds of 3 components of WDR neurons, increasing intensities of electrical stimulus (0.1–3 mA, 0.5 ms pulse width) was applied at the muscular RFs during extracellular recording (Figure 3A). Conduction velocity (CV) of different afferent fibers was calculated through dividing the distance between stimulus and recording site (about 0.12 m) by the latency, without regard to the synaptic delays occurring within the SDH. Elicited discharges of WDR neurons were shown in Figure 3B and Table 1. A β - was the fastest component (CV, 12.24 \pm 8.86 m/s) with lowest threshold ($T_{A\beta}$, 0.53 \pm 0.06 mA) and shortest latency (12.60 \pm 4.97 ms). A δ - was the slower component (CV, 3.36 \pm 1.57 m/s) with higher threshold ($T_{A\delta}$, 0.90 \pm 0.26 mA) and longer latency (44.26 \pm 23.24 ms). C- was the slowest component (CV, 1.07 \pm 0.28 m/s) with highest threshold (T_C , 2.06 \pm 0.13 mA) and longest latency (117.88 \pm 35.61 ms). Accordingly, intensity of $T_{A\beta}$, $T_{A\delta}$, T_C and $2T_C$ was determined as 0.5 mA, 1 mA, 2 mA and 4 mA in later experiments, respectively.

Nociceptive Discharges of WDR Neurons Elicited by HS

After identification of the general properties of WDR neurons, the nociceptive discharges were elicited by injection of HS at left gastrocnemius muscle of rats (Figure 4A). As expected, 11 WDR neurons from 9 rats exhibited robust discharges immediately after HS injection, while no firing was evoked by 0.9% NaCl (Figure 4B and C). Since the discharges of

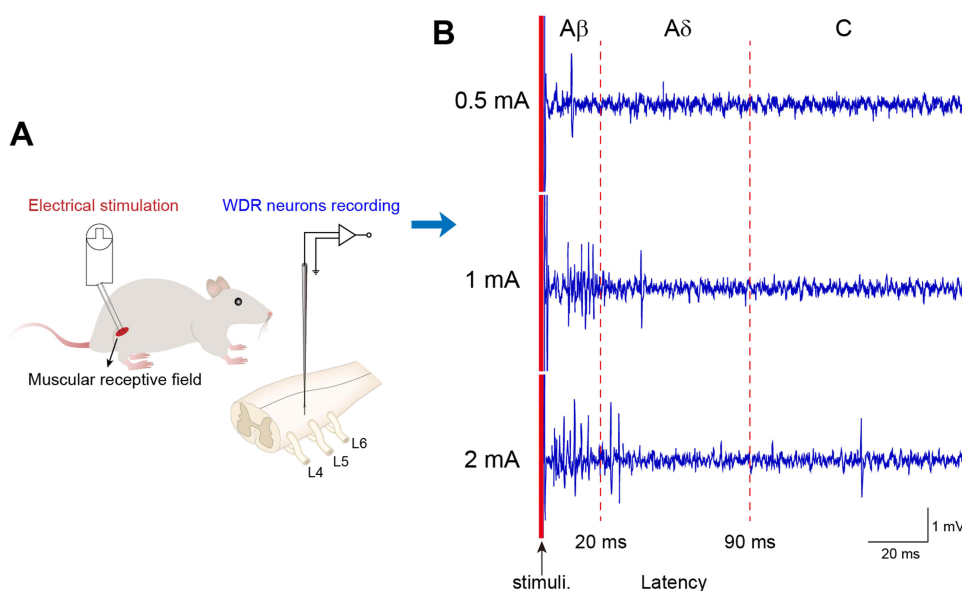


Figure 3 Intensity thresholds of electrical stimulation activating Aβ, Aδ and C-components of WDR neurons.
Notes: (A) Schematic diagram of experimental setup. Electrical stimulation (0.1–3 mA, 0.5 ms) was applied at muscular RFs of WDR neurons and action potentials of WDR neurons were recorded by a microelectrode inserted in the enlargement of spinal cord. (B) Representative discharges of Aβ (0–20 ms latency), Aδ (20–90 ms latency) and C (90–300 ms latency) components of WDR neurons evoked by electrical stimulation with intensity of 0.5, 1 and 2 mA, respectively (9 neurons from 7 rats).

WDR neurons induced by HS exhibited short duration and decreased rapidly, the firing rates during the 1st 1 min after injection were further analyzed. The discharge frequency gradually decreased over time. During the 1st 20s it was 28.3 ± 11.6 Hz, but it decreased sharply to 16.2 ± 10.5 Hz in the 3rd 20s ($P < 0.05$, Figure 4C). Further analysis of firing rates of WDR neurons in the 1st 20s course showed that a majority of WDR neurons (55%) fired at a rate of 20–30 Hz, 18% WDR neurons fired at 10–20 Hz, and 27% WDR neurons fired at 30–60 Hz (Figure 4D). Therefore, the activities of WDR neurons within the 1st 20s after HS were selected to be observed.

Effects of Pre-EA at RFs on Nociceptive Discharges of WDR Neurons Evoked by HS

There were quite a number of WDR neurons with RFs located at both gastrocnemius muscle and anterior tibial muscle. Pre-EA of $T_{A\beta}$ (0.5 mA), $T_{A\delta}$ (1 mA), T_C (2 mA) or $2T_C$ (4 mA) was administered at left anterior tibial muscle. Immediately after pre-EA intervention, HS was applied to the ipsilateral gastrocnemius muscle. Nociceptive activities of WDR neurons were compared to evaluate the effects of pre-EA with distinct intensities at RFs. Figure 5A displayed representative firing traces of WDR neurons in 4 EA groups. Compared with the model group (28.3 ± 11.6 Hz), pre-EA of $T_{A\delta}$ (8.92 ± 4.26 Hz, $P < 0.05$), T_C (10.20 ± 6.50 Hz, $P < 0.05$) and $2T_C$ (6.62 ± 3.04 Hz, $P < 0.01$) significantly reduced discharge frequencies of WDR neurons (Figure 5B), with suppressive rates of 68.48%, 63.96% and 76.61%, respectively. However, pre-EA of $T_{A\beta}$ had no inhibitory effect

Table 1 Identification of the Threshold, Latency, and CV of Aβ-, Aδ- and C-Components of WDR Neurons (9 Neurons from 7 Rats) by Electrical Stimulation

Component	Threshold (mA)	Latency (ms)	CV (m/s)
Aβ-	0.53 ± 0.06	12.60 ± 4.97	12.24 ± 8.86
Aδ-	0.90 ± 0.26	44.26 ± 23.24	3.36 ± 1.57
C-	2.06 ± 0.13	117.88 ± 35.61	1.07 ± 0.28

Abbreviation: CV, conduction velocity.

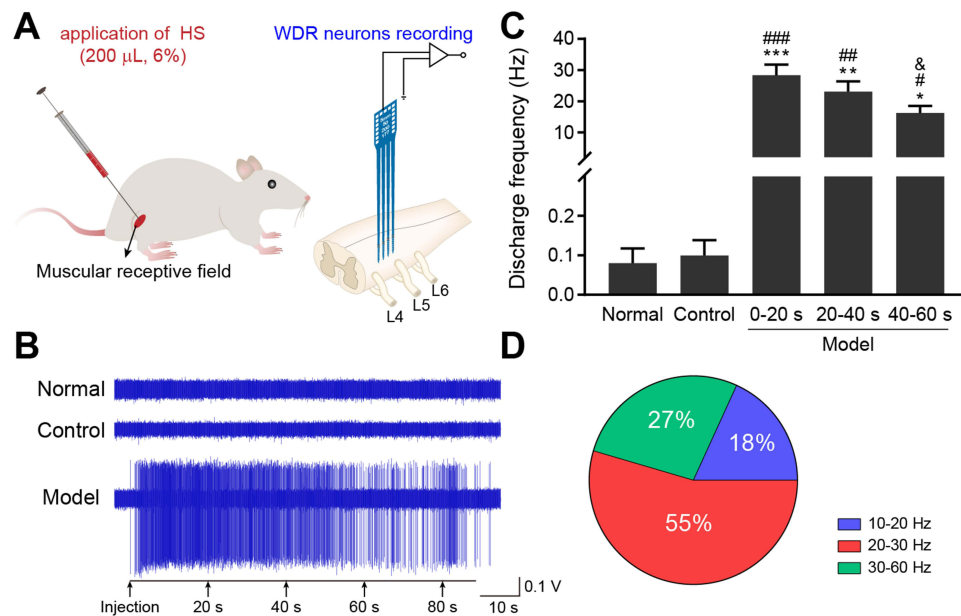


Figure 4 Injection of hypertonic saline (HS) at RFs evoked robust discharges of WDR neurons.

Notes: (A) Schematic diagram of experimental setup. 200 μ L HS was injected at gastrocnemius muscle and action potential of WDR neurons was recorded by a microelectrode array inserted in L5-6 segment of spinal cord. (B) Representative traces of discharges of WDR neurons in the 3 groups. (C) Discharge frequency of WDR neurons in the 3 groups. Frequency of model group was further analyzed during 0–20, 20–40 and 40–60 s post-injection of HS (5 neurons from 3 rats in normal group, 6 neurons from 3 rats in control group, 11 neurons from 9 rats in model group). (D) Percentages of WDR neurons with different discharge frequency after injection of HS within 20s (11 neurons from 9 rats). All data were presented as means \pm SEM. *, $P < 0.05$, ** $P < 0.01$, *** $P < 0.001$. #, compared with normal, # $P < 0.05$, ## $P < 0.01$, ### $P < 0.001$. & Compared with 0–20s, &#mathP < 0.05.

on WDR neurons. These results suggested that pre-EA administered at the RFs required A δ - or C- afferents to inhibit nociceptive responses of WDR neurons.

Effects of Pre-EA at Adjacent Non-RFs on Nociceptive Discharges of WDR Neurons

WDR neurons that responded to mechanical stimulation only on the gastrocnemius muscle but not the anterior tibial muscle were observed in this part. Likewise, pre-EA of 4 intensities was administered at left anterior tibial muscle (identified as adjacent non-RFs) and HS was applied to the ipsilateral gastrocnemius muscle. As shown in Figure 5C and D, discharge frequency of WDR neurons in T $_{A\beta}$ (11.9 ± 5.37 Hz, $P < 0.05$), T $_{A\delta}$ (9.32 ± 7.66 Hz, $P < 0.05$), T $_C$ (9.43 ± 2.85 Hz, $P < 0.05$) and 2T $_C$ (4.32 ± 4.46 Hz, $P < 0.01$) groups decreased significantly compared with that of the model (Figure 5D). The inhibition rate of 4 groups was 57.95%, 67.06%, 66.68% and 84.73%, respectively. These results indicated that pre-EA at adjacent non-RFs could effectively inhibit the nociceptive activities of WDR neurons, especially pre-EA of T $_{A\beta}$. The other intensities of pre-EA at adjacent non-RFs produced the same effects as that in the RFs.

Effects of Pre-EA at Contralateral Non-RFs on Nociceptive Discharges of WDR Neurons

It has been reported that heterotopic EA intervention can elicit extrasegmental analgesia.^{7,29} Meanwhile, the activities of the WDR neurons could be inhibited by heterotopic stimulation with high intensity in different pain models of rats.^{30,31} Here, we examined the effective intensity of pre-EA at right anterior tibial muscle (contralateral non-RFs) which suppressed nociceptive firing of WDR neurons in an acute muscle pain model. Interestingly, pre-EA of T $_C$ and 2T $_C$ remarkably reduced HS-evoked WDR neuronal activities to 7.49 ± 4.70 Hz and 6.25 ± 6.74 Hz, and the inhibiting rate was 73.53% and 77.92%, respectively (Figure 6, $P < 0.01$). However, no obvious alleviation was observed for pre-EA with the intensity of T $_{A\delta}$ (13.58 ± 5.07 Hz, Figure 6, $P > 0.05$) and T $_{A\beta}$ (15.74 ± 5.36 Hz, Figure 6, $P > 0.05$) on firing frequency of WDR neurons. Overall, these results indicated that intensity of heterotopic pre-EA intervention should reach at least T $_C$ to suppress nociceptive discharges of WDR neurons.

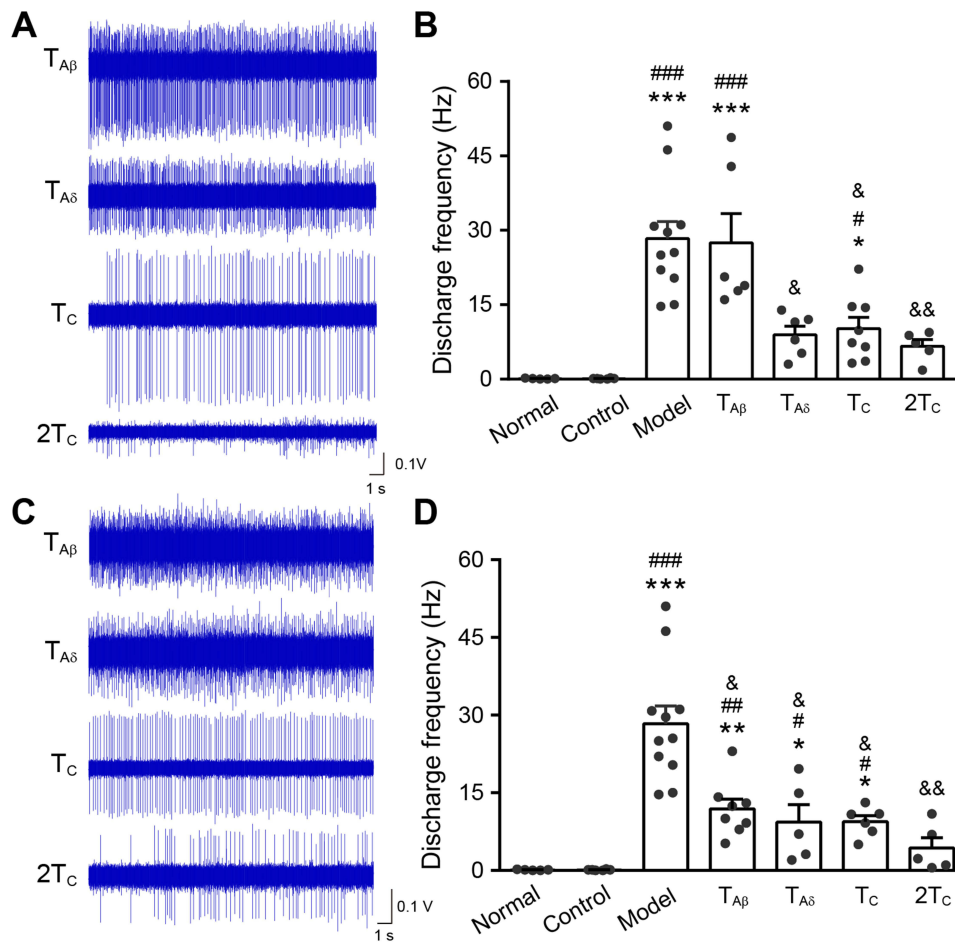


Figure 5 Changes of noxious firing of WDR neurons after pre-EA at ipsilateral RFs or non-RFs with different intensities.

Notes: (A, B) Representative discharge traces (A) and frequency (B) of WDR neurons after pre-EA at ipsilateral RFs (6 neurons from 3 rats in T_{Aβ} group, 6 neurons from 4 rats in T_{Aδ} group, 8 neurons from 3 rats in T_C group, 5 neurons from 4 rats n=5 in 2T_C group). (C, D) Representative discharge traces (C) and frequency (D) of WDR neurons after pre-EA at ipsilateral non-RFs (8 neurons from 8 rats in T_{Aβ} group, 5 neurons from 4 rats in T_{Aδ} group, 6 neurons from 3 rats in T_C group, 5 neurons from 3 rats in 2T_C group). All data were presented as means ± SEM. *, compared with normal, *P < 0.05, **P < 0.01, ***P < 0.001. #Compared with control, #P < 0.05, ##P < 0.01, ###P < 0.001. &Compared with model, &P < 0.05, &&P < 0.01.

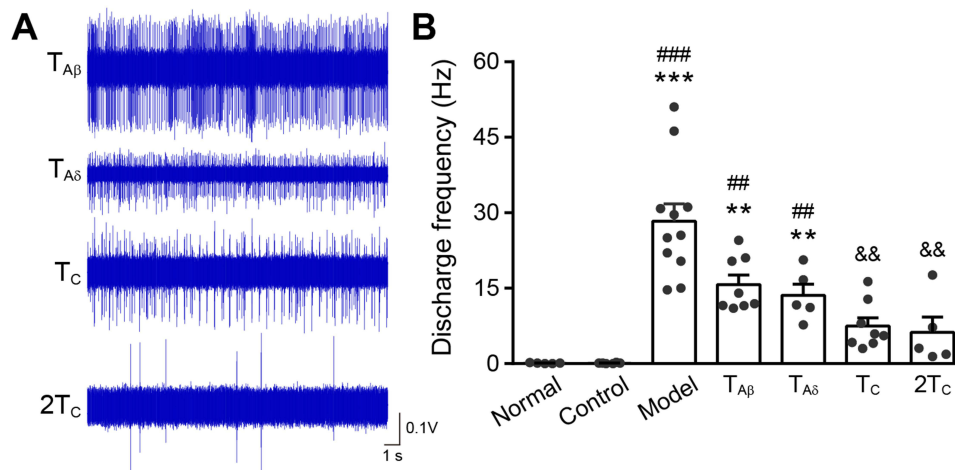


Figure 6 Changes of activity of WDR neurons after contralateral pre-EA with different intensities.

Notes: (A) Representative traces of discharge of WDR neurons in the 4 groups. (B) Discharge frequency of WDR neurons in the 7 groups (8 neurons from 6 rats in T_{Aβ} group, 5 neurons from 4 rats in T_{Aδ} group, 8 neurons from 3 rats in T_C group, 5 neurons from 3 rats in 2T_C group). All data were presented as means ± SEM. *, compared with normal, **P < 0.01, ***P < 0.001. #Compared with control, #P < 0.01, ##P < 0.001. &Compared with model, &&P < 0.01.

Discussion

In the present study, the inhibitory effects of pre-EA with distinct intensities and locations on nociceptive discharges of WDR neurons were compared. Specifically, pre-EA of $T_{A\beta}$, $T_{A\delta}$, T_C or $2T_C$ at ipsilateral adjacent non-RFs could inhibit nociceptive discharges of WDR neurons, while in local RFs, only $T_{A\delta}$, T_C or $2T_C$ of pre-EA could exert inhibitory effects. Meanwhile, at contralateral non-RFs, intensity of pre-EA should reach at least T_C to suppress discharges of WDR neurons. These results suggested that pre-EA could inhibit nociceptive activities of WDR neurons and the effective intensities varied depending on the locations of stimulation.

Intramuscular injection of HS is commonly used to evoke acute muscle pain.^{32–34} Application of HS at gastrocnemius muscle induced mechanical hyperalgesia^{35,36} and c-Fos expression in deep (IV–VI) lamina of SDH of L4–6 segments.^{37,38} In this study, WDR neurons in deep lamina IV–VI of SDH exhibited obvious discharges, indicating that WDR neurons were activated following intramuscular injection of HS. Interestingly, pretreatment of EA effectively inhibits nociceptive activities of WDR neurons and the effects were dependent on intensities and locations of intervention, showing the preventive analgesic effects of pre-EA.

Behavior and electrophysiological evidence have demonstrated that activation of low-threshold mechanoreceptors could alleviate pain symptoms and inhibit the spontaneous discharges of dorsal horn neurons.^{39–42} This analgesic effect has been generally explained by the gate control theory, which suggests that the nociceptive ($A\delta/C$) inputs are gated by feed-forward activation of non-nociceptive ($A\beta$) afferents in SDH. The spinal WDR neurons receive inputs from both non-nociceptive ($A\beta$) and noxious ($A\delta$ and C) afferents.⁴³ Activation of A-fibers inhibited the nociceptive discharges of WDR neurons evoked by C-fiber.⁴⁴ In addition, the underlying mechanisms of the segmental analgesia of acupuncture have been suggested to be associated with the gate control theory.^{10,16,45} In this study, pre-EA with low intensity $T_{A\beta}$ inhibited nociceptive discharges of WDR neurons, indicating that anti-nociceptive effects of pre-EA may also be related to the gate control theory. However, the phenomena only occurred when pre-EA with $T_{A\beta}$ was administered at adjacent non-RFs. As we know, there are also inhibitory fields (adjacent non-RFs) around the excitatory fields (known as RFs) of WDR neurons.⁴⁶ It was demonstrated that tactile stimulus of adjacent non-RFs could reduce the activities of WDR neurons to nociceptive stimulation.^{47–49} That is why pre-EA of $T_{A\beta}$ at non-RFs was effective rather than at RFs. Besides, pre-EA of $T_{A\delta}$ at both RFs and non-RFs was effective on the nociceptive firing of WDR neurons.

Apart from local acupoints, contralateral or distal acupoints are also frequently used to relieve pain.^{7,50,51} Different from segmental analgesia induced by homotopic acupoint, systemic analgesia by heterotopic acupoints requires relatively higher intensity which is enough to activate myelinated fibers (thinly $A\delta$ - and/or C -fibers).^{9,52,53} Mechanisms underlying systemic AA involve the diffuse noxious inhibitory controls (DNICs),^{54–57} which refer to the strong inhibitory effects on spinal WDR neurons by a nociceptive stimulus applied to any part of the body distinct from their RFs.⁵⁸ In the present study, heterotopic nociceptive afferent stimulation by pre-EA inhibited nociceptive discharges of WDR neurons, indicating the information was convergent and integrated by WDR neurons. Specifically, ipsilateral pre-EA with high intensity ($T_{A\delta}$, T_C or $2T_C$) significantly decreased discharge frequency of WDR neurons. While at contralateral non-RFs, only intensity higher than T_C could generate inhibitory effects on WDR neurons. This was consistent with a previous study which reported that threshold of $A\delta$ -fiber activation showed less effective when administered at contralateral acupoints.¹¹ Consequently, these results implied that inhibitory effects of pre-EA with high intensity on nociceptive discharges of WDR neurons may be through DNIC pathway, and the extent to which DNIC was triggered varied with distinct intensities.

Activation of different somatic afferents play important roles in AA. Previous studies determined the intensity of EA by recordings of nociceptive reflexes (RIII reflex).^{10,11,16} As the C-fiber reflex was a kind of nociceptive response,^{59,60} it was difficult to find out the threshold of $A\beta$ -fiber. Other studies employed single-unit recording of primary afferent fibers or sensory neurons to determine the intensity.^{25,45,61} In the present study, to better investigate the inhibitory effects of pre-EA on spinal WDR neurons, it was more reliable to determine the intensities of EA by thresholds of the 3 components of WDR neurons. Moreover, this measurement may reveal the integration of pre-EA and nociceptive signaling in the dorsal horn.

However, the present study has some limitations. We only analyzed discharges of WDR neurons by in vivo electrophysiological recording, further study is needed to evaluate whether pre-EA could relieve acute pain behavior. Additionally, we merely examined the effects of pre-EA at spinal level. Supraspinal components may also participate in this complex loop, especially in systemic analgesia of heterotopic pre-EA. Further studies should be performed to elucidate the supraspinal mechanisms of antinociceptive effects of pre-EA with distinct intensities.

Conclusion

In summary, different afferent stimulation of pre-EA and nociceptive information were convergent and integrated by WDR. Pre-EA with distinct intensities inhibits noxious discharges of WDR neurons depending on the locations of stimulation. Our studies suggest novel therapeutic strategies for parameters' selection of pre-EA for acute pain.

Acknowledgments

This work was supported by grants from the National Natural Science Foundation of China (82130122, 81973964). The experiment platform was provided by Institute of Acupuncture and Moxibustion, China Academy of Chinese Medical Sciences.

Disclosure

The authors declare that the research was conducted in the absence of any commercial or financial relationships that could be construed as a potential conflict of interest.

References

- Jessri M, Sultan AS, Tavares T, Schug S. Central mechanisms of pain in orofacial pain patients: implications for management. *J Oral Pathol Med.* 2020;49(6):476–483.
- Ikeda A, Muroki A, Suzuki C, Shimazu Y, Takeda M. Resolvin D1 suppresses inflammation-induced hyperexcitability of nociceptive trigeminal neurons associated with mechanical hyperalgesia. *Brain Res Bull.* 2020;154:61–67.
- Ito H, Toyota R, Takeda M. Phytochemical quercetin alleviates hyperexcitability of trigeminal nociceptive neurons associated with inflammatory hyperalgesia comparable to NSAIDs. *Mol Pain.* 2022;18:17448069221108971.
- Sadeghi M, Manaheji H, Zaringhalam J, et al. Evaluation of the GABAA receptor expression and the effects of muscimol on the activity of wide dynamic range neurons following chronic constriction injury of sciatic nerve in rats. *Basic Clin Neurosci.* 2021;12(5):651–666.
- Zain M, Bonin RP. Alterations in evoked and spontaneous activity of dorsal horn wide dynamic range neurons in pathological pain: a systematic review and analysis. *Pain.* 2019;160(10):2199–2209.
- Coghill RC, Mayer DJ, Price DD. Wide dynamic range but not nociceptive-specific neurons encode multidimensional features of prolonged repetitive heat pain. *J Neurophysiol.* 1993;69(3):703–716.
- Zhu J, Xu Q, Zou R, et al. Distal acupoint stimulation versus peri-incisional stimulation for postoperative pain in open abdominal surgery: a systematic review and implications for clinical practice. *BMC Complement Altern Med.* 2019;19(1):192.
- Lv ZT, Shen LL, Zhu B, et al. Effects of intensity of electroacupuncture on chronic pain in patients with knee osteoarthritis: a randomized controlled trial. *Arthritis Res Ther.* 2019;21(1):120.
- Zhao ZQ. Neural mechanism underlying acupuncture analgesia. *Prog Neurobiol.* 2008;85(4):355–375.
- Xin J, Su Y, Yang Z, et al. Distinct roles of ASIC3 and TRPV1 receptors in electroacupuncture-induced segmental and systemic analgesia. *Front Med.* 2016;10(4):465–472.
- Zhu B, Xu WD, Rong PJ, Ben H, Gao XY. A C-fiber reflex inhibition induced by electroacupuncture with different intensities applied at homotopic and heterotopic acupoints in rats selectively destructive effects on myelinated and unmyelinated afferent fibers. *Brain Res.* 2004;1011(2):228–237.
- Acar HV. Acupuncture and related techniques during perioperative period: a literature review. *Complement Ther Med.* 2016;29:48–55.
- Yuan W, Wang Q. Perioperative acupuncture medicine: a novel concept instead of acupuncture anesthesia. *Chin Med J.* 2019;132(6):707–715.
- Qu Z, Liu L, Yang Y, et al. Electro-acupuncture inhibits C-fiber-evoked WDR neuronal activity of the trigeminocervical complex: neurophysiological hypothesis of a complementary therapy for acute migraine modeled rats. *Brain Res.* 2020;1730:146670.
- Fan Y, Kim DH, Gwak YS, et al. The role of substance P in acupuncture signal transduction and effects. *Brain Behav Immun.* 2021;91:683–694.
- Duan-Mu CL, Zhang XN, Shi H, et al. Electroacupuncture-induced muscular inflammatory pain relief was associated with activation of low-threshold mechanoreceptor neurons and inhibition of wide dynamic range neurons in spinal dorsal horn. *Front Neurosci.* 2021;15:687173.
- Zhou T, Wang J, Han CX, Torao I, Guo Y. Analysis of interspike interval of dorsal horn neurons evoked by different needle manipulations at ST36. *Acupunct Med.* 2014;32(1):43–50.
- Hong S, Ding S, Wu F, et al. Strong manual acupuncture manipulation could better inhibit spike frequency of the dorsal horn neurons in rats with acute visceral nociception. *Evid Based Complement Alternat Med.* 2015;2015:675437.
- Yu L, Wang W, Li L, et al. Inhibition of electroacupuncture on nociceptive responses of dorsal horn neurons evoked by noxious colorectal distention in an intensity-dependent manner. *J Pain Res.* 2019;12:231–242.
- Cui JJ, Wang J, Xu DS, et al. Alexa Fluor 488-conjugated cholera toxin subunit B optimally labels neurons 3–7 days after injection into the rat gastrocnemius muscle. *Neural Regen Res.* 2022;17(10):2316–2320.

21. Zhang Z, Xu D, Wang J, et al. Correlated sensory and sympathetic innervation between the acupoint BL23 and kidney in the rat. *Front Integr Neurosci*. 2020;14:616778.
22. Xue M, Sun YL, Xia YY, Huang ZH, Huang C, Xing GG. Electroacupuncture modulates spinal BDNF/TrkappaB signaling pathway and ameliorates the sensitization of dorsal horn WDR neurons in spared nerve injury rats. *Int J Mol Sci*. 2020;21:18.
23. Urch CE, Dickenson AH. In vivo single unit extracellular recordings from spinal cord neurones of rats. *Brain Res Brain Res Protoc*. 2003;12(1):26–34.
24. Greenspon CM, Battell EE, Devonshire IM, Donaldson LF, Chapman V, Hathway GJ. Lamina-specific population encoding of cutaneous signals in the spinal dorsal horn using multi-electrode arrays. *J Physiol*. 2019;597(2):377–397.
25. Fang Y, Zhu J, Duan W, Xie Y, Ma C. Inhibition of muscular nociceptive afferents via the activation of cutaneous nociceptors in a rat model of inflammatory muscle pain. *Neurosci Bull*. 2020;36(1):1–10.
26. Kakita K, Tsubouchi H, Adachi M, Takehana S, Shimazu Y, Takeda M. Local subcutaneous injection of chlorogenic acid inhibits the nociceptive trigeminal spinal nucleus caudalis neurons in rats. *Neurosci Res*. 2018;134:49–55.
27. Rezaee L, Manaheji H, Haghparast A. Role of spinal glial cells in excitability of wide dynamic range neurons and the development of neuropathic pain with the L5 spinal nerve transection in the rats: behavioral and electrophysiological study. *Physiol Behav*. 2019;209:112597.
28. Yang F, Xu Q, Cheong YK, et al. Comparison of intensity-dependent inhibition of spinal wide-dynamic range neurons by dorsal column and peripheral nerve stimulation in a rat model of neuropathic pain. *Eur J Pain*. 2014;18(7):978–988.
29. Youssef AM, Macefield VG, Henderson LA. Pain inhibits pain; human brainstem mechanisms. *Neuroimage*. 2016;124(Pt A):54–62.
30. Lapirot O, Chebbi R, Monconduit L, Artola A, Dallel R, Luccarini P. NK1 receptor-expressing spinoparabrachial neurons trigger diffuse noxious inhibitory controls through lateral parabrachial activation in the male rat. *Pain*. 2009;142(3):245–254.
31. Meléndez-Gallardo J, Eblen-Zajjur A. Noxious mechanical heterotopic stimulation induces inhibition of the spinal dorsal horn neuronal network: analysis of spinal somatosensory-evoked potentials. *Neurol Sci*. 2016;37(9):1491–1497.
32. Norbury R, Smith SA, Burnley M, Judge M, Mauger AR. The effect of elevated muscle pain on neuromuscular fatigue during exercise. *Eur J Appl Physiol*. 2021;1:548.
33. Asiri YI, Fung DH, Fung T, et al. A new hypertonic saline assay for analgesic screening in mice: effects of animal strain, sex, and diurnal phase. *Can J Anaesth*. 2021;68(5):672–682.
34. Larsen DB, Graven-Nielsen T, Hirata RP, Boudreau SA. Differential corticomotor excitability responses to hypertonic saline-induced muscle pain in forearm and hand muscles. *Neural Plast*. 2018;2018:7589601.
35. Lei J, Jin L, Zhao Y, et al. Sex-related differences in descending norepinephrine and serotonin controls of spinal withdrawal reflex during intramuscular saline induced muscle nociception in rats. *Exp Neurol*. 2011;228(2):206–214.
36. Lei J, Sun T, Lumb BM, You HJ. Roles of the periaqueductal gray in descending facilitatory and inhibitory controls of intramuscular hypertonic saline induced muscle nociception. *Exp Neurol*. 2014;257:88–94.
37. Panneton WM, Gan Q, Ariel M. Injections of algescic solutions into muscle activate the lateral reticular formation: a nociceptive relay of the spinoreticulothalamic tract. *PLoS One*. 2015;10(7):e0130939.
38. Chen YK, Lei J, Jin L, Tan YX, You HJ. Dynamic variations of c-Fos expression in the spinal cord exposed to intramuscular hypertonic saline-induced muscle nociception. *Eur J Pain*. 2013;17(3):336–346.
39. Jones MG, Rogers ER, Harris JP, et al. Neuromodulation using ultra low frequency current waveform reversibly blocks axonal conduction and chronic pain. *Sci Transl Med*. 2021;13:608.
40. Sdrulla AD, Xu Q, He SQ, et al. Electrical stimulation of low-threshold afferent fibers induces a prolonged synaptic depression in lamina II dorsal horn neurons to high-threshold afferent inputs in mice. *Pain*. 2015;156(6):1008–1017.
41. Staud R, Robinson ME, Goldman CT, Price DD. Attenuation of experimental pain by vibro-tactile stimulation in patients with chronic local or widespread musculoskeletal pain. *Eur J Pain*. 2011;15(8):836–842.
42. Mancini F, Nash T, Iannetti GD, Haggard P. Pain relief by touch: a quantitative approach. *Pain*. 2014;155(3):635–642.
43. Craig AD. Pain mechanisms: labeled lines versus convergence in central processing. *Annu Rev Neurosci*. 2003;26:1–30.
44. Woolf CJ, Wall PD. Chronic peripheral nerve section diminishes the primary afferent A-fibre mediated inhibition of rat dorsal horn neurones. *Brain Res*. 1982;242(1):77–85.
45. Chen L, Wang X, Zhang X, et al. Electroacupuncture and moxibustion-like stimulation relieves inflammatory muscle pain by activating local distinct layer somatosensory afferent fibers. *Front Neurosci*. 2021;15:695152.
46. Le Bars D. The whole body receptive field of dorsal horn multireceptive neurones. *Brain Res Brain Res Rev*. 2002;40(1–3):29–44.
47. Hillman P, Wall PD. Inhibitory and excitatory factors influencing the receptive fields of lamina 5 spinal cord cells. *Exp Brain Res*. 1969;9(4):284–306.
48. Salter MW, Henry JL. Physiological characteristics of responses of wide dynamic range spinal neurones to cutaneously applied vibration in the cat. *Brain Res*. 1990;507(1):69–84.
49. Salter MW, Henry JL. Differential responses of nociceptive vs. non-nociceptive spinal dorsal horn neurones to cutaneously applied vibration in the cat. *Pain*. 1990;40(3):311–322.
50. Wong L, Wan D, Wang Y. Local and distant acupuncture points stimulation for chronic musculoskeletal pain: a systematic review on the comparative effects. *Eur J Pain*. 2015;19(9):1232–1247.
51. Peng Y, You H, Chen X, et al. Effect of electroacupuncture at homotopic and heterotopic acupoints on abdominal pain in patients with irritable bowel syndrome: study protocol for a randomized controlled trial. *Trials*. 2018;19(1):559.
52. Kagitani F, Uchida S, Hotta H. Afferent nerve fibers and acupuncture. *Auton Neurosci*. 2010;157(1–2):2–8.
53. Xu WD, Zhu B, Rong PJ, Bei H, Gao XY, Li YQ. The pain-relieving effects induced by electroacupuncture with different intensities at homotopic and heterotopic acupoints in humans. *Am J Chin Med*. 2003;31(5):791–802.
54. Le Bars D, Dickenson AH, Besson J-M. Diffuse noxious inhibitory controls (DNIC). I. effects on dorsal horn convergent neurones in the rat. *Pain*. 1979;6(3):283–304.
55. Le Bars D, Dickenson AH, Besson J-M. Diffuse noxious inhibitory controls (DNIC). II. lack of effect on non-convergent neurones, supraspinal involvement and theoretical implications. *Pain*. 1979;6(3):305–327.

56. Cummins TM, Kucharczyk MM, Graven-Nielsen T, Bannister K. Activation of the descending pain modulatory system using cuff pressure algometry: back translation from man to rat. *Eur J Pain*. 2020;24(7):1330–1338.
57. Yuan XC, Zhu B, Jing XH, et al. Electroacupuncture potentiates cannabinoid receptor-mediated descending inhibitory control in a mouse model of knee osteoarthritis. *Front Mol Neurosci*. 2018;11:112.
58. Villanueva L, Le Bars D. The activation of bulbo-spinal controls by peripheral nociceptive inputs: diffuse noxious inhibitory controls. *Biol Res*. 1995;28(1):113–125.
59. Zhi MJ, Liu K, Zheng ZL, et al. Application of the chronic constriction injury of the partial sciatic nerve model to assess acupuncture analgesia. *J Pain Res*. 2017;10:2271–2280.
60. Radek RJ, Curzon P, Decker MW. Supraspinal and systemic administration of the nicotinic-cholinergic agonist (\pm)-epibatidine has inhibitory effects on C-fiber reflexes in the rat. *Brain Res Bull*. 2004;64(4):323–330.
61. Huo R, Han SP, Liu FY, et al. Responses of primary afferent fibers to acupuncture-like peripheral stimulation at different frequencies: characterization by single-unit recording in rats. *Neurosci Bull*. 2020;36(8):907–918.

Journal of Pain Research

Dovepress

Publish your work in this journal

The Journal of Pain Research is an international, peer reviewed, open access, online journal that welcomes laboratory and clinical findings in the fields of pain research and the prevention and management of pain. Original research, reviews, symposium reports, hypothesis formation and commentaries are all considered for publication. The manuscript management system is completely online and includes a very quick and fair peer-review system, which is all easy to use. Visit <http://www.dovepress.com/testimonials.php> to read real quotes from published authors.

Submit your manuscript here: <https://www.dovepress.com/journal-of-pain-research-journal>